

Liquid-Crystalline Elastomers Containing Sulfonic Acid Groups

Bao-Yan Zhang,* Fan-Bao Meng, Bao-Ling Zang, and Jian-she Hu

Department of Chemistry, Northeastern University, 110004, Shenyang, P.R. China

Received August 15, 2002; Revised Manuscript Received February 12, 2003

ABSTRACT: A series of ionic liquid-crystalline (LC) elastomers were synthesized by using chemical cross-linking agents containing sulfonic acid groups, which were siloxane-based materials. A ionic divinyl monomer 2,2'-(1,2-ethenediyl)bis[5-[(4-undecenoxy)phenyl]azo]benzenesulfonic acid was used as chemical cross-linking agent. Cholest-5-en-3-ol(3 β)-10-undecenoate was synthesized as a liquid-crystalline monomer. The effective cross-link density of the ionic elastomers was determined by swelling experiments in organic/buffer mixtures. Their liquid-crystalline properties were characterized by DSC, POM, and SAXS. A proposed multilayer buildup containing LC segment structure and ionic cross-linking lamellar structure separated by siloxane chains was given. The ion aggregated in domains forces the siloxane chains to fold and form an irregular lamellar structure. The ionic cluster lamellae may be tangled with the rigid mesogenic groups of LC segments to form multiple blocks. Liquid-crystal mesophase region of the polymers become narrow with increasing ionic cross-linking content.

Introduction

Liquid-crystalline (LC) elastomers have received a lot of interest during recent years owing to their special optical, mechanical and piezoelectric properties.^{1–3} The polymer network structure of the LC elastomers is usually produced by the introduction of cross-linking into liquid-crystalline polymer systems. This cross-linking results in materials with a number of unusual properties.

Recently research has been extended to polymers having ionic and mesogenic sites in their chain.⁴ The ionic groups are incorporated either into the molecular backbone or on side chains to improve the physical properties and water dispersibility of hydrophobic organic polymers.⁵ The introduction of the ionic species was found to affect the properties of the liquid-crystalline polymers.⁶ Ionic aggregates can play a role in physical cross-linking and provide an important and characteristic viscoelastic behavior of ionomers. Strong ionic interactions between polymer molecules are known to significantly enhance mechanical properties, which include compressive strength.⁷ On the other hand, the incorporation of small concentration of ions into organic polymers has been shown to lead to microphase-separated ionic domains that influence greatly the properties of the polymers.

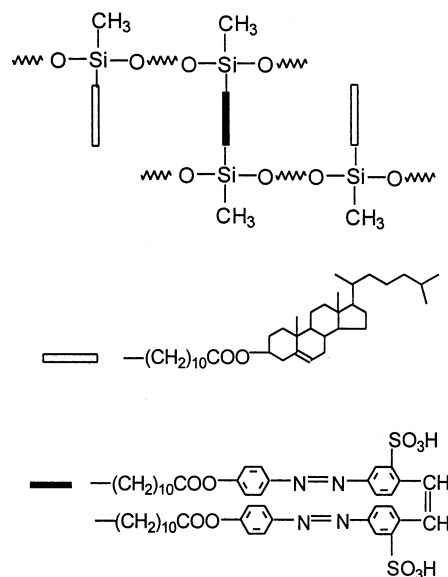
Amphiphilic networks which exhibit both hydrophilic and hydrophobic properties have attracted a lot of attention because of their interesting physical properties as well as their potential technological applications.⁸

However, little work has been reported on the effect of chemical cross-linking agents containing ionic groups on the properties of liquid-crystalline networks.

One would like to know the fundamental link between ionic aggregation found in the networks and the behavior of liquid-crystalline phases. Furthermore, it is of interest to investigate how the ionic interactions modify liquid crystallinity, liquid-crystalline structure, and properties of such kinds of elastomers.

* To whom correspondence should be addressed. E-mail: baoyanzhang@hotmail.com.

Scheme 1



In the present study, we prepared a series of liquid-crystalline elastomers using chemical cross-linking agents containing ionic groups, which were siloxane-based materials. Their general structure is shown in Scheme 1. Elastomers of this type may be readily prepared in a one-step reaction, in which both the mesogenic unit and a ionic divinyl monomer added to the polymer backbone.

Experimental Section

Material and Measurements. 10-Undecylenoic acid, brilliant yellow, cholesterol, and pyridine were purchased from Beijing Chemical Co. Hexachloroplatinic acid hydrate and thionyl chloride were obtained from Shenyang Chemical Co. Poly(methylhydrogen)siloxane (PMHS) was provided by Merck. Pyridine was purified by distillation over KOH and NaH before using.

FTIR spectra of the synthesized polymers and monomers in the solid state were obtained by the KBr method performed on a Nicolet 510P FTIR spectrometer.

Thermal transition properties were characterized by a TA Instruments Q100 at a heating rate of 10 °C/min under

Table 1. Polymerization and Photoluminescence Properties

sample	feed				yield (%)	photoluminescence ^a	
	PMHS (mmol)	A (mmol)	B (mmol)	A/(A + B) (mol %)		λ_{\max} (nm)	intens ^b ($\times 10^3$)
P ₀	0.3	0	9.00	0	92	494	0.17
P ₁	0.3	0.023	8.96	0.25	90	493	0.37
P ₂	0.3	0.045	8.91	0.50	88	494	1.89
P ₃	0.3	0.090	8.82	1.00	87	493	3.90
P ₄	0.3	0.225	8.55	2.56	85	492	8.21
P ₅	0.3	0.450	7.20	11.1	80	493	12.1
P ₆	0.3	0.900	0.00	100	80	493	12.1
P ₇	0.3	4.500	0.00	100	80	493	12.1

^a Obtained from solutions of the samples (0.0050 g) in 50 mL toluene. ^b Calculated by the peak area.

nitrogen atmosphere. Visual observation of liquid crystalline transitions under cross polarized light was made by a Leitz Laborlux S polarizing optical microscope (POM) equipped with a THMS-600 heating stage.

The photoluminescence (PL) spectra of the monomer and polymers was obtained using a Shanghai Instruments Model-960 Spectrofluorophotometer.

Small-angle X-ray scattering (SAXS) measurements were performed using Cu K α ($\lambda = 1.542 \text{ \AA}$) radiation monochromatized with a Ni filter and a totally reflecting glass block (Huber small-angle chamber 701). The intensity curves were measured using a linear position sensitive detector (Mbraun OED-50 M).

Syntheses. Synthesis of 2,2'-(1,2-Ethenediyl)bis[5-[(4-undecenoxy)phenyl]azo]benzenesulfonic Acid. 10-Undecylenic acid (18.4 g, 0.1 mol) and thionyl chloride (25.0 g, 0.21 mol) were added into a round flask equipped with an absorption instrument of hydrogen chloride. The mixture was stirred at room temperature for 2 h, then heated to 60 °C, and kept for 3 h in a water bath to ensure that the reaction finished. The mixture was distilled under reduced pressure to obtain 12.4 g of 10-undecenoyl chloride at 160–170 °C (20 mmHg) in the yield of 61%.

Brilliant yellow (6.3 g, 0.01 mol) was dissolved in 120 mL of pyridine to form a solution. 10-undecenoyl chloride (4.1 g, 0.02 mol) was added to the solution and reacted at 80 °C for 6 h, cooled, poured into 500 mL of cold water and acidified with 6 N H₂SO₄. The precipitated crude product was filtered and recrystallized from ethanol/water (1/1) and dried overnight at 85 °C under vacuum to obtain a brown powder of product in the yield of 70%. Mp: above 300 °C.

IR (KBr, cm⁻¹): 3420(–OH); 3080(=C–H); 1760(C=O); 1600(N=N); 1500(C=C); 1121(S=O in –SO₃H).

Synthesis of Cholest-5-en-3-ol(3 β)-10-undecenoate. To a solution of cholesterol (19.3 g, 0.50 mol) in 100 mL of pyridine was added 10-undecenoyl chloride (11.0 g, 0.054 mol) and reacted at reflux temperature for 3 h. The mixture was dispersed in H₂O (500 mL) and acidified with 6 N HCl. The precipitated crude product was filtered and recrystallized from ethanol. The product was dried under vacuum to obtain a white powder, cholest-5-en-3-ol(3 β)-10-undecenoate, in a yield of 80%.

IR (KBr, cm⁻¹): 3050(=C–H); 2965–2854(CH₃– and –CH₂–); 1735(C=O).

Synthesis of the Elastomers. For synthesis of polymers P₀–P₇, the same method was adopted. The polymerization experiments are summarized in Table 1. The synthesis of polymer P₂ was given as an example. 2,2'-(1,2-Ethenediyl)bis[5-[(4-undecenoxy)phenyl]azo]benzenesulfonic acid (0.042 g, 0.045 mmol, monomer A) was dissolved in 60 mL of dry, fresh distilled toluene. To the stirred solution were added cholest-5-en-3-ol(3 β)-10-undecenoate (4.92 g, 8.91 mmol, monomer B), poly(methylhydrogen)siloxane (0.63 g, 0.30 mmol), and 2 mL of H₂PtCl₆/THF (0.50 g hexachloroplatinic acid hydrate dissolved in 100 mL of tetrahydrofuran THF), and this mixture was heated under nitrogen and anhydrous conditions at 65 °C for 48 h. The solvent was removed under reduced pressure, and the crude polymer was purified by precipitation from

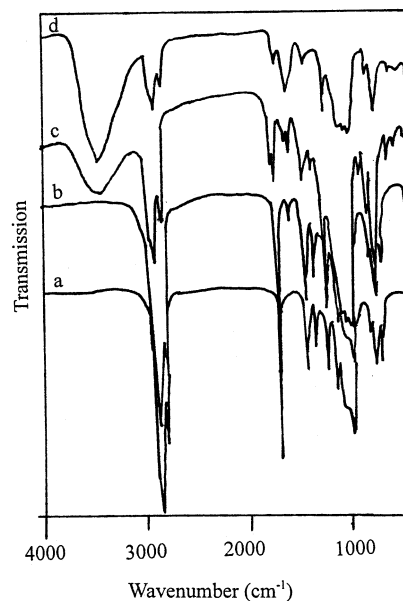


Figure 1. IR spectra for (a) P₀, (b) P₂, (c) P₆, and (d) P₇.

solution in methanol by the addition of THF. After filtration and evaporation of the solvent, the product was dried at 80 °C for 2 h under vacuum to obtain 5.03 g of polymer in a yield of 90%.

IR(KBr, cm⁻¹): 2960–2850 (CH₃– and –CH₂–); 1608 (N=N); 1738(C=O).

Results and Discussion

FTIR Spectra. Figure 1 shows the FTIR spectra of nonionic LC polymer P₀, ionic LC polymers P₂ and P₆, and ionic polymer P₇ recorded at room temperature in KBr pellets. The disappearance of the Si–H stretching at 2160 cm⁻¹ indicates successful incorporation of monomers into the polysiloxane chains. Polymer P₆ contains the representative features for all of the ionic liquid-crystalline elastomers, their characteristic absorption bands are as follows: 3424 (O–H stretching), 2932, 2857 (C–H aliphatic), 1738 and 1755 (C=O stretching in two kinds of ester modes), 1608 (N=N stretching), and 845 cm⁻¹ (=C–H out-of-plane bending). The FTIR absorption bands of the C=O stretching vibration (1734 cm⁻¹ in P₀; 1757 cm⁻¹ in P₇) indicate different ester linkage.

For organic sulfonic acid, the FTIR absorption range of the O=S=O asymmetric and symmetric stretching modes lies in 1100–1260 and 1010–1080 cm⁻¹ respectively. Because of the overlap found for both asymmetric and symmetric stretching bands of SO₂ with C–O and Si–O stretching bands in the polymers under study, the N=N stretching mode in bright yellow group is chosen for identification of ionic groups in the polymers. Because of the symmetric structure of aromatic groups, their C=C stretching vibrations are weak. FTIR peaks at 1600 cm⁻¹ should be regarded as the N=N stretching mode. Figure 1 compares the FTIR spectra for (a) nonionic P₀, (b) 0.5 mol % ionic content P₂, (c) 11.1 mol % ionic content P₆, and (d) ionic polymer P₇. While there is no N=N stretching mode found in nonionic content P₀, such a mode is found as a weak band at 1600 cm⁻¹ for the sample of 0.5 mol % ionic content, and stronger absorption bands are found at 1597 and 1600 cm⁻¹ for the samples of P₆ and P₇. These results clearly indicate successful incorporation of ionic groups, whose concen-

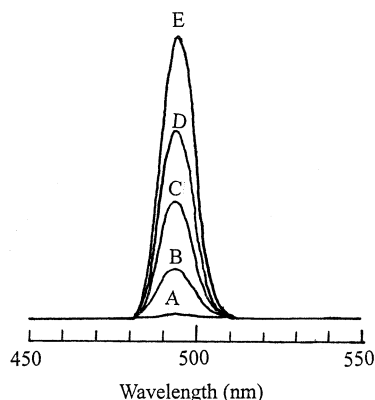


Figure 2. PL spectra for (A) P₀, (B) P₂, (C) P₄, (D) P₆, and (E) P₇ in toluene at the same concentration.

tration increases with an increase in the concentration of ionic monomers containing bright yellow content.

Photoluminescence (PL) Spectra. Because of the azo groups and the conjugated structure, the ionic cross-linking agent of the elastomers can be analyzed by using PL spectrum. Figure 2 shows the PL spectra of the elastomers, which were obtained from a solution of the elastomer (0.0500 g) in 50 mL of toluene. It is shown that the photoluminescent maxima of the ionic elastomers occur at about 493 nm. The spectra are narrow because of the constant chromophores in the elastomers. The intensities of the peaks increase linearly with increasing ionic monomer concentration in the feed (Table 1).

Swelling Behavior. There are several ways to determine the effective cross-link density (or the molecular weight between the cross-link points (M_c)) of a polymer network. Most commonly used are the methods of measuring the rubber elasticity or the swelling characteristics. We have studied these elastomers with the help of swelling experiments.

Amphiphilic networks exhibit both hydrophilic and hydrophobic properties, so organic/water mixtures were chosen as swelling solvent. Because of the nature of the pH-sensitive ionic elastomers, the solvents were selected by the percentage swelling of elastomer P₄ in THF/buffer, dimethyl sulfoxide (DMSO)/buffer, and acetone/buffer. The buffer solution of pH 3.1 was composed of 0.20 M HAc and 0.004 M NaAc.

Dried networks sample (of approximately 0.2 g each) were placed in the bottom of 20 mL glass bottles. An accurately known large initial volume of a solvent mixture was added. After the bottles were sealed, they were left in a constant temperature insulated box for 2 days. The fully swollen networks were then blotted with filter paper to remove the surface solvent before weighing. The percentage swelling of these samples was defined as (swollen weight/dried weight) \times 100%. To determine preferential absorption in solvent mixtures, it was necessary to use smaller volume of solvent in the swelling tests. Figure 3 depicts the swelling behavior for elastomer P₄ in three mixture solvents. It was shown that the swelling ratio of elastomer P₄ is largest for DMSO/buffer, followed by THF/buffer and then acetone/buffer. So the swelling measurements were made in DMSO/buffer solvent.

Swelling measurements were made in 10 mL of DMSO/buffer mixtures (volume ratio 1/1) with samples of about 0.2 g in initial weight. A buffer solution of desired pH and ionic strength I (0.1 M) was used as a

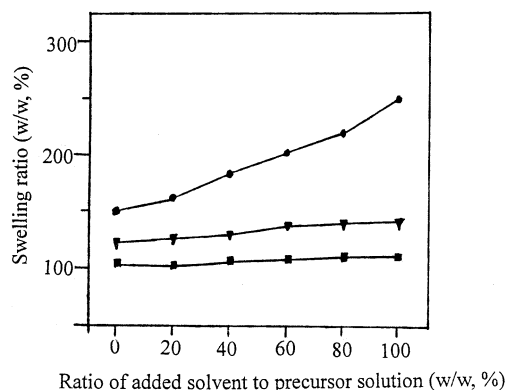


Figure 3. Swelling ratio (swollen weight/dry weight) of P₄ in different solvents: (-■-) in acetone/buffer; (-●-) in DMSO/buffer; (-▼-) in THF/buffer.

function of solvent composition. The buffer solutions of different pH values were made by the Britton–Pobinson method. Swelling was accomplished in several days at room temperature. Swollen elastomers removed from solvents at regular intervals were dried superficially with filter paper, weighed and placed in the same condition. The measurements were continued until a constant weight was reached for each sample.

The equilibrium/swelling ratio of networks was determined gravimetrically through the following equation:

$$Q = 1 + (W_2/W_1 - 1)\rho_p/\rho_s \quad (1)$$

where Q is the swelling ratio of networks by volume, W_1 is the weight of the network before swelling, W_2 is the weight of the network at equilibrium swelling; ρ_p and ρ_s are densities of polymer and solvent, respectively. The volume fraction of polymer network V_{2S} was calculated as

$$V_{2S} = 1/Q \quad (2)$$

The density of the polymer networks was determined in absolute ethyl alcohol by measuring the exact volume of the sample (~ 1 g). The values of the density of ethyl alcohol and their dependence on temperature were taken from literature.⁹

Ionic polymer networks in aqueous solutions yield a more complicated situation than that of neutral polymers. When the networks contain ionizable groups, the forces that influence swelling may be greatly increased. The Flory–Rehner models,¹⁰ which describe the molecular weight between cross-links, can only be applied to homogeneous networks. The ionic elastomers do not fall in this category. Brannon–Peppas derived an equation to describe this ionic contribution term for both anionic and cationic systems.¹¹

$$V_1 [K_a/(10^{-\text{pH}} + K_a)]^2 (V_{2S}/V)^2/4I = [\ln(1 - V_{2S}) + V_{2S} + \chi V_{2S}^2] + [V_1/(VM_c)](1 - 2M_c/M_n) \times V_{2r} [(V_{2S}/V_{2r})^{1/3} - (V_{2S}/V_{2r})/2] \quad (3)$$

where M_c is the number-average molecular weight between cross-links, χ is the Flory polymer–swelling agent interaction parameter, V_1 is the molar volume of the swelling agent, I is the ionic strength of the swelling medium, K_a is the dissociation constant of ionizable groups on polymer, V is the specific volume of dry

Table 2. Some Swelling Properties of the Polymers

sample	density (g/cm ³)	<i>V</i> (cm ³ /g)	<i>V</i> _{2r}	<i>V</i> _{2S}				<i>χ</i>	<i>M</i> _c (g/mol)
				pH 1.9	pH 2.4	pH 3.5	pH 4.5		
P ₀	1.063	0.94							
P ₁	1.069	0.94	0.99	0.30	0.30	0.29	0.20	0.614	4800
P ₂	1.078	0.93	0.99	0.33	0.33	0.32	0.22	0.624	4000
P ₃	1.083	0.92	0.98	0.33	0.33	0.32	0.23	0.630	3500
P ₄	1.101	0.91	0.97	0.34	0.34	0.33	0.24	0.636	3000
P ₅	1.117	0.90	0.95	0.40	0.40	0.39	0.30	0.656	2500
P ₆	1.129	0.89	0.94	0.50	0.51	0.50	0.40	0.739	1200
P ₇	1.150	0.87	0.92						

polymer, *M*_n is the number-average molecular weight of the linear macromolecules before cross-linking; and *V*_{2r} is the polymer volume fraction after cross-linking but before swelling.

Using eq 3, we can obtain a linear relation with *χ* and *M*_c values as the intercept and inverse slope, respectively, as expressed by eq 4

$$A = \chi + B/M_c \quad (4)$$

where *A* and *B* are defined as

$$A = \{V_1[K_a/(10^{-pH} + K_a)]^2(V_{2S}/V)^2/4I - \ln(1-V_{2S}) - V_{2S} + 2V_1V_{2r}[(V_{2S}/V_{2r})^{1/3} - (V_{2S}/V_{2r})/2]/(VM_n)\}/V_{2S}^2 \quad (5)$$

$$B = V_1V_{2r}[(V_{2S}/V_{2r})^{1/3} - (V_{2S}/V_{2r})/2]/(VV_{2S}^2) \quad (6)$$

The relevant experimental parameters to be used are as follows: *I* = 0.1 M, *V*₁ = 28.7 cm³/mol, *M*_n = 20 100, p*K*_a = 6.0. The parameter *V* is calculated by using density values of the polymers. Some of the information about the structural properties of the elastomers was collected in Table 2. By using both the experimentally measured polymer volume fractions *V*_{2S} of the elastomers in their equilibrium-swollen state and the above-mentioned data, we can calculate the values of *A* and *B*. By using the values of *A* and *B*, it is possible to establish the corresponding linear relationships about *χ* and 1/*M*_c, as shown in Figure 4. The respective *χ* and *M*_c values were determined via linear regression analysis of the lines given in Figure 4, which are listed in Table 2.

From the results listed in Table 2 one can see that for the ionic network with the lowest amount of cross-linking agents relatively high values for the degree of swelling are found. For the cross-link density, although we used the Brannon-Peppas formula rather than the Flory-Rehner expression, it is also shown that an increase in the molecular weight between cross-links increases the swelling of the polymer.

Liquid-Crystalline Behavior. All the polymers were studied by DSC and observed by polarizing microscopy, which data are summarized in Table 3.

Figure 5 shows the DSC thermograms of all the polymers synthesized. In the DSC curves, the soft segment glass transition (*T*_g) is easily discernible at about 9 °C in P₀, and it increases with increasing cross-linking content. It increases slowly from P₀ to P₄ and from P₅ to P₇, but it increases sharply from P₄ to P₅. The melting temperature (*T*_m) of the crystalline polymers is clearly detected in P₀, P₁, P₂, P₃, and P₄. From P₀ to P₃, the values of *T*_m decrease with increasing cross-linking content, whereas the enthalpy of melting in-

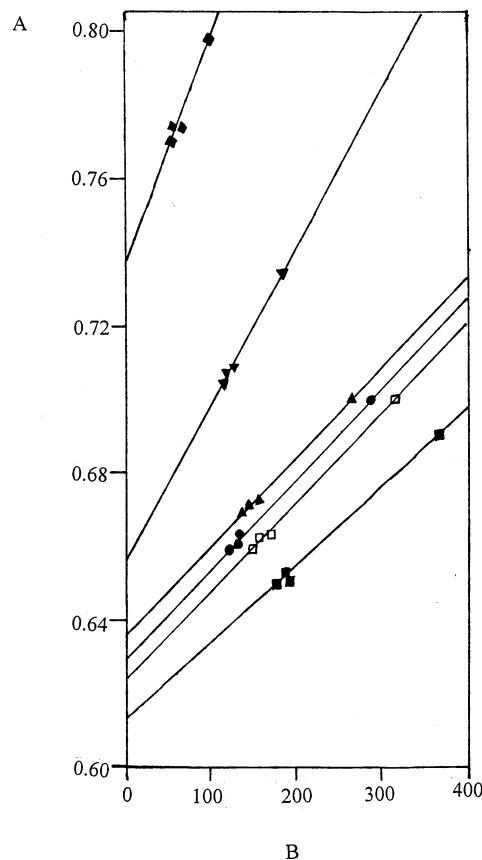


Figure 4. Determination of *χ* and *M*_c values of polymers from swelling data: (■) for P₁; (□) for P₂; (●) for P₃; (▲) for P₄; (▼) for P₅; (◆) for P₆.

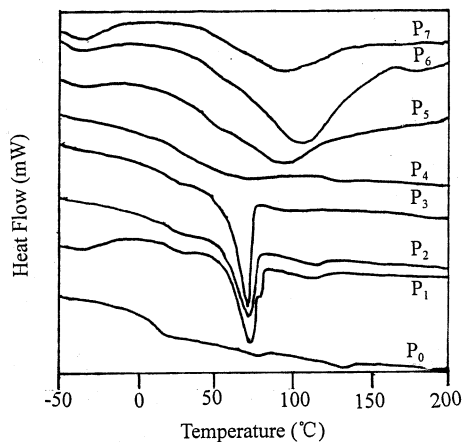
Table 3. Thermal Properties of Series Polymers

sample	DSC			optical microscope	
	<i>T</i> _g ^a (°C)	<i>T</i> _m ^b (°C)	<i>T</i> _i ^c (°C)	<i>T</i> _m ^b (°C)	<i>T</i> _i ^c (°C)
P ₀	9	76	131	78	140
P ₁	18	74	115	74	120
P ₂	22	71	113	72	117
P ₃	24	68	98	70	103
P ₄	26	75	136	76	137
P ₅	49	91		92	
P ₆	50	106		106	
P ₇	51	93			

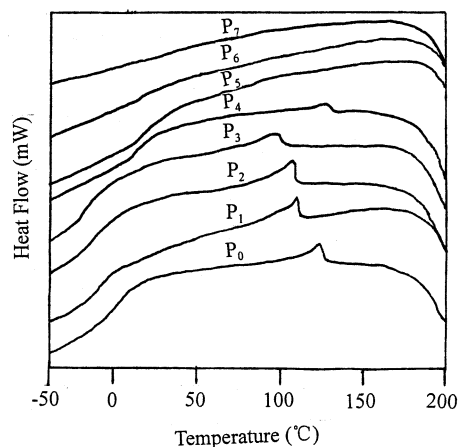
^a Glass transition temperature of siloxane matrix. ^b Melting temperature of crystalline polymers. ^c Meso-to-isotropic phase transition temperature of mesogenic segments.

creases. Because endothermic peaks of P₅ and P₆ were very broad, transition temperatures were determined by optical polarizing microscope observations. In the DSC curves, the anisotropic-to-isotropic transition temperature (*T*_i) of the polymers is found in P₀–P₄, whereas in samples P₅–P₇ it could not be detected. For P₅ and P₆, the anisotropic-to-isotropic phase transition was not seen by optical polarizing microscope observations. The liquid-crystal mesophase region decreases with increasing cross-linking content from P₀ to P₃. For P₅ and P₆, which contain more ionic cross-linking content, the liquid-crystal mesophase disappears. The polymer P₄ is a particular polymer which possess liquid-crystal mesophase with proper ionic cross-linking content.

The optical polarizing microscope observations revealed that the polymers containing LC content exhibited smectic mesophase textures (except P₅ and P₆). Figure 6 shows mesophase textures of the representa-



(A)



(B)

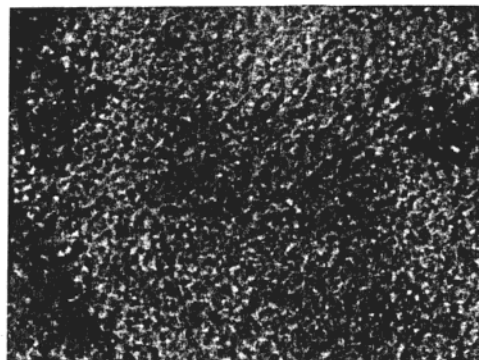
Figure 5. DSC thermograms of series polymers: (A) on the first heating (10 °C/min), (B) on the first cooling (10 °C/min).

tive polymer P₂ on first heating. When it was heated on the hot stage of the polarizing microscope, a broken focal-conic fan-shaped texture appeared. When heating continued to 72 °C, the focal-conic fan-shaped texture of the smectic A phase appeared. When heating to 117 °C, eyeshot became dark demonstrating the anisotropic-to-isotropic phase transition.

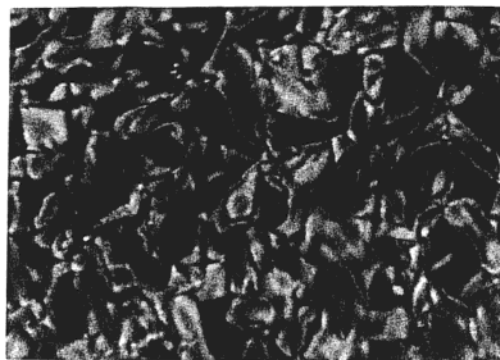
Both ionic groups and chemical cross-linking may influence the liquid-crystalline behavior of the elastomers.

Liquid crystalline polymers are most commonly composed of flexible and rigid moieties; self-assembly and nanophase separation into specific microstructures (often lamellar for side chain architecture) frequently occur due to geometric and chemical dissimilarity of the two moieties. The majority of side-chain liquid-crystalline polymers such as siloxane polymers are atactic; for such disordered systems, low temperatures induce vitrification rather than crystallization. For polymer of this type, the glass-transition temperature may be considered as a measure of the backbone flexibility. In addition, the nature of the side group also influences the glass-transition temperature.

Chemical cross-linking imposes additional constraints on the segmental motion of polymer chains, and might be expected to raise the glass-transition temperatures. However, it illustrates a general principle that low level of cross-linking do not markedly effect the phase be-



(A)



(B)

Figure 6. Optical polarizing micrographs of polymer P₂ at (A) 65 and (B) 72 °C on first heating (200 \times).

havior of the materials.¹² Cross-linking units may act as a nonmesogenic diluent and destabilize the phase in a manner analogous to the freezing-point depression in liquids. Furthermore, chemical cross-links in polymers could introduce inhomogeneity in the networks in the form of clustered hard segments.

It is well-known that the incorporation of ionic groups leads to an elevated glass transition temperature for ionomers based on amorphous, flexible polymers.^{13,14} On the other hand, ionic side-chain polymers lead to nanophase-separated morphologies.¹⁵ For ionomers with a relatively low proportion of ionic units, two-phase behavior is frequently observed due to ionic aggregation in a relatively nonpolar matrix, with consequent reduction in mobility of neighboring nonpolar regions.

In this scheme, at lower ionic contents, ion pairs exist as small ionic aggregates, called multiplets, as well as isolated ion pairs. These multiplets work as ionic cross-links and raise the T_g . As the ionic content increases, an ion-rich phase, called a cluster phase, begins to form and increases its volume. The cluster phase is considered to be a separate phase.¹⁶ Cluster aggregation in which the ion clusters are completely surrounded with the organic material and actual microseparation of the ionic phase from the siloxane matrix takes place. On the other hand, poly(methylsiloxane) has low glass transition temperature; the phase separation process should thus be fast because the siloxane matrix has high mobility.¹⁷ Obviously the organization of the longer hard segments is easier, resulting in a higher degree of crystallinity of the hard phase. These results demonstrate the enthalpy of melting increases in P₁, P₂, and P₃ (containing 0.25%, 0.5%, and 1.0% ionic cross-linking content, respectively).

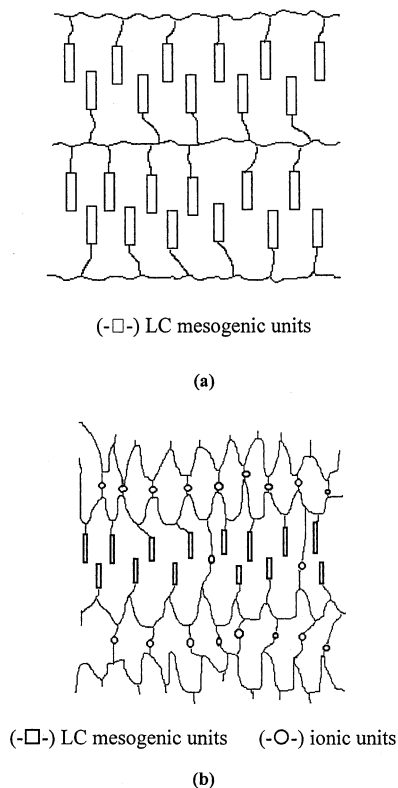


Figure 7. Proposed structure of the polymers for (a) P_0 and (b) ionic elastomers.

The ion aggregate in domains due to their electrostatic interactions, thus forcing the siloxane chains to fold and form an irregular lamellar structure. These lamellae are similar to some crystalline–amorphous block copolymers. The ionic clusters lamellae are parallel to LC mesogenic layer at lower ionic contents.

A proposed multilayer buildup containing LC segment structure and ionic cross-linking lamellar structure separated by siloxane chains is represented schematically in Figure 7b.

In the ionomer literature, the soft and hard phases are also frequently referred to the matrix phase and the cluster phase, respectively. Ionic aggregates or multiplets may be dispersed in the soft or matrix phase. The hard or cluster phase is essentially composed of complex aggregates of multiplets along with a considerable proportion of nonionic material whose mobility is significantly reduced, thus leading to a higher T_g than the soft or matrix phase.¹⁸

For P_5 and P_6 , an increased broadening of melting peaks with an increase in the ionic content is seen from DSC thermograms (see Figure 5). These results should reflect increased diversity in size and in the arrangement of crystallites, possibly due to increased structural heterogeneity. The ionic cluster lamellae may be tangled with the rigid mesogenic groups of LC segments to form multiple blocks, leading to the disappearance of liquid-crystal mesophases. These results also demonstrate it is difficult to observe T_i .

These results are confirmed by small-angle X-ray scattering (SAXS). The scattering vector lies in the horizontal direction, and its length is defined as

$$q = (4\pi/\lambda) \sin \theta \quad (7)$$

where 2θ is the scattering angle and λ is the wavelength of the radiation. The scattering peaks were detected in

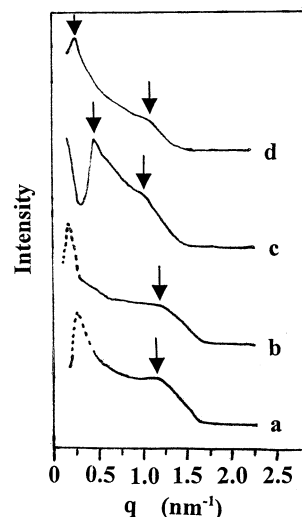


Figure 8. SAXS patterns collected from the series of polymers for (a) P_0 , (b) P_3 , (c) P_5 , and (d) P_6 .

the SAXS profiles of as-cast films of P_0 , P_3 , P_5 , and P_6 at 25 °C as illustrated in Figure 8.

For the polymer P_0 , besides intense peak corresponding to a characteristic size of 252 Å (which is due to crystallinity (the long spacing)), a shoulder peak at $q = 1.27 \text{ nm}^{-1}$ is observed, and the derived Bragg spacing (d) is 50 Å. The presence of the shoulder peak at small scattering angles suggests the layered packing of the mesogenic groups. The microstructure of the polymer P_0 is most likely lamellar in nature. Compared to the calculated molecular length (l) of 32 Å for the fully extended side-chain liquid-crystalline unit, the lamellae thickness ($d = 50 \text{ Å}$) is less than twice of the calculated molecular length ($l < d < 2l$). A reasonable proposed packing arrangement is shown schematically in Figure 7a.

For the polymer P_3 which contains a small amount of ionic cross-linking content, the X-ray scattering pattern is similar to the profile of P_0 . The long spacing of P_3 is 284 Å, whereas P_0 is 252 Å. The increased number of higher order reflections is attributed to the crystallization effect of ionic aggregates. It suggests the organization of the longer hard segments is easier, resulting in a higher degree of crystallinity of the hard phase.

As shown in Figure 8, the X-ray scattering pattern of P_5 shows an intense scattering peak at $q = 0.45 \text{ nm}^{-1}$ and a shoulder peak at $q = 0.98 \text{ nm}^{-1}$, which suggests the long period of P_5 , 140 Å. The two reflections suggest a lamellar structure. A proposed way to incorporate ionic aggregates into the mesogens microstructure is by nanophase separation of the ionic aggregates and mesogenic units, such that each lamellae is composed of a mesogenic sublayer and an ionic aggregates sublayer, as illustrated in Figure 7b. The thickness of the layered packing of mesogenic groups is about 50 Å for P_0 and P_3 . On the other hand, the calculated molecular length (l) of the fully extended ionic cross-linking unit is about 76 Å. In consideration of the thickness of the soft main-chain matrix, the long period (140 Å) of P_5 is sum of the thickness of the mesogenic layer and the ionic clusters lamellae. For P_5 , this result is in agreement with the proposed model.

For P_6 , the profiles show an intense peak at $q = 0.23 \text{ nm}^{-1}$ (corresponding to a characteristic size of 276 Å) and a shoulder peak at $q = 1.02 \text{ nm}^{-1}$. The thickness

(276 Å) of the sample is much greater than the sum of the thickness of mesogenic layers and ionic aggregates. It indicates that the ionic clusters lamellae may be tangled with the rigid mesogenic groups of LC segments to form multiple blocks.

Conclusions

We have synthesized a series of liquid-crystalline elastomers using chemical cross-linking agents containing sulfonic acid groups, which were siloxane-based materials. A ionic divinyl monomer 2,2'-(1,2-ethenediyl)-bis[5-(4-undecenyloxy)phenyl]azo]benzenesulfonic acid was used as chemical cross-linking agent. Cholest-5-en-3-ol(β)-10-undecenoate was synthesized as a liquid-crystalline monomer. The polymers were prepared in a one-step reaction with ionic cross-linking contents ranging between 0 and 100 mol %. Their chemical structures were determined by various experimental techniques including FTIR and PL spectroscopies. Their liquid-crystalline properties were characterized by DSC, POM, and SAXS. We have studied the elastomers with the help of swelling experiments to determine the effective cross-link density (M_c). Ionic polymer networks in aqueous solutions yield a more complicated situation than that of homogeneous networks. We employed the Brannon-Peppas expression instead of Flory-Rehner models. The variety of network structures obtained by varying the ionic cross-linking contents leads to different swelling properties in mixed buffer/organic solvent mixtures.

A proposed multilayer buildup containing LC segment structure and ionic cross-linking lamellar structure separated by siloxane chains was given. The ion aggregated in domains forces the siloxane chains to fold and form an irregular lamellar structure. Under the condition that there is a small amount of ionic cross-linking content in LC elastomers, the organization of the longer hard segments is easier, resulting in some different properties for LC polymers. A proposed way to incorporate ionic aggregates into the mesogens microstructure is by nanophase separation of the ionic aggregates and mesogenic units, such that each lamellae is composed of a mesogenic sublayer and an ionic aggregates sublayer. As the ionic content increases greatly, the ionic cluster lamellae may be tangled with the rigid mesogenic groups of LC segments to form multiple blocks. The liquid-crystal mesophase region of the polymers becomes narrower with increasing ionic cross-linking content.

LC elastomers combine the properties of the LC phase (the combination of order and mobility) with rubber elasticity. Their most outstanding characteristic is their

mechanical orientability; strains as small as 20% are enough to obtain a perfectly oriented LC domain. On the other hand, it is known that strong ionic interactions (bonds) between polymer chains can significantly enhance mechanical properties, which include compressive strength. In ionic polymers, polymer chains are ionically cross-linked through nondirectional ionic bonds, which are strong but are thermally labile. Thus, unlike chemically cross-linked polymers, they melt upon heating and reform upon cooling.

Ionic LC elastomers would combine the mechanical properties of ionic polymers with the mechanical orientability properties of conventional LC elastomers, resulting in new technological applications. The mechanical properties and stress-induced orientation will be studied later.

Acknowledgment. The authors are grateful to the National Natural Scientific Fundamental Committee of China and the Minister of Science and Technology of China for financial support of this work.

References and Notes

- (1) Mitchell, G. R.; Davis, F. J.; Guo, W.; Cywinski, R. *Polymer* **1991**, *32*, 1347.
- (2) Kupfer, J.; Finkelmann, H. *Macromol. Chem., Rapid Commun.* **1991**, *12*, 717.
- (3) Meier, W.; Finkelmann, H. *Macromol. Chem., Rapid Commun.* **1990**, *11*, 599.
- (4) Ujtie, S.; Iimura, K. *Macromolecules* **1992**, *25*, 3174.
- (5) Navratil, M.; Eisenberg, A. *Macromolecules* **1974**, *7*, 84.
- (6) Zhang, B. Y.; Weiss, R. A. *J. Polym. Sci., Part A: Polym. Chem.* **1992**, *30*, 91.
- (7) Eisenberg, A.; King, M. *Ion-containing polymers*; Academic Press: New York, 1977.
- (8) Kim, J.-Y.; Cohen, C. *Macromolecules* **1998**, *31*, 3542.
- (9) *Handbook of Chemistry and Physics*; CRC Press: Boca Raton, FL.
- (10) Flory, P. J.; Rehner, J. J. *J. Chem. Phys.* **1943**, *11*, 521.
- (11) Brannon-Peppas, L.; Peppas, N. A. *Chem. Eng. Sci.* **1991**, *46*, 715.
- (12) Frederick, J. D. *J. Mater. Chem.* **1993**, *3* (6), 551.
- (13) Holliday, L. In *Ionic polymers*; Holliday, L., Ed.; Applied Science: London, 1975; Chapter 1.
- (14) Hara, M.; Sauer, J. A. *J. Macromol. Sci., Rev. Macromol. Chem. Phys.* **1994**, *C34*, 325.
- (15) Plate, N. A.; Shibaev, V. P. *J. Polym. Sci., Macromol. Rev.* **1974**, *8*, 117.
- (16) Eisenberg, A.; Hird, B.; Moore, R. B. *Macromolecules* **1990**, *23*, 4098.
- (17) Graiver, D.; Litt, M.; Baer, E. *J. Polym. Sci., Polym. Chem. Ed.* **1979**, *17*, 3573.
- (18) Eisenberg, A.; Kim, J. S. *Introduction to Ionomers*; John Wiley & Sons: New York, 1998. Schlick, S., Ed.; *Ionomers: Characterization, Theory and Applications*; CRC Press: Boca Raton, FL, 1996.

MA021333E